Journal of The Electrochemical Society, **157** (6) A735-A740 (2010)
0013-4651/2010/157(6)/A735/6/$28.00 © The Electrochemical Society

Overcharge Protection for 4 V Lithium Batteries at High Rates and Low Temperatures

Guoying Chen*,z and Thomas J. Richardson*

Environmental Energy Technologies Division, Lawrence Berkeley National Laboratory, Berkeley, California 94720, USA

Overcharge protection for 4 V $Li_{1.05}Mn_{1.95}O_4$/lithium cells at charging rates in excess of 1 mA/cm^2 (3C) and at temperatures of as low as −20°C was achieved using a bilayer separator coated with two electroactive polymers. High rate and low temperature overcharge protection and discharge performance were improved by employing a design in which the polymer-coated portion of the separator is in parallel with the cell rather than between the electrodes. The effects of different membrane supports for the electroactive polymers were also examined.
© 2010 The Electrochemical Society. [DOI: 10.1149/1.3392370] All rights reserved.

Manuscript submitted February 22, 2010; revised manuscript received March 16, 2010. Published April 28, 2010.

Rechargeable lithium batteries are known for their high energy density and excellent cycle life, and they have become the dominant technology for personal electronic devices. Safety issues persist, however, with numerous unfortunate incidents reported in recent years. Overcharging has long been recognized as a primary problem, as dangerous events involving fire and explosion can result.[1] For vehicle applications (with low tolerance for hazards), series-connected cells are required to provide high voltages. Monitoring and controlling the potential of individual cells within the stack presents a severe challenge in terms of weight, volume, and cost. An alternative approach that provides reliable and inexpensive protection is needed to maintain each cell within a safe potential window. Extension of cell pack lifetime is an additional benefit.

Redox shuttle additives have been studied extensively for this purpose.[2-4] That approach is fundamentally limited, however, as it relies on the diffusion of additive molecules and radical cations across the separator, resulting in low rate capability and poor low temperature performance. Because lithium ion batteries are especially susceptible to damage on overcharging at low temperatures due to high resistances in both electrodes and electrolyte[5] and because vehicle batteries are unavoidably exposed to low temperatures, an alternative (or additional) protection mechanism is needed.

We have previously demonstrated the use of electroactive polymers to provide overcharge protection for rechargeable lithium batteries.[6] When impregnated into a porous membrane separator, a small amount of polymer can provide self-actuated, reversible protection for cells using a variety of chemistries. Detailed characterization and modeling of the protection mechanism has provided useful cell design parameters.[7,8] A bilayer configuration comprising a high voltage polymer composite adjacent to the cathode and a low voltage polymer composite adjacent to the battery anode expands applicability to cells that operate above 4 V vs Li.[9] Because the polymer protection approach uses electronic conduction and only a minimum of ion mobility is required to establish the internal short, it is relatively immune to limitations imposed by charging rate and low temperatures. In this paper, we demonstrate the high rate capability and excellent low temperature performance of an electroactive polymer overcharge protection, using an overcharge-susceptible lithium-rich spinel $Li_{1.05}Mn_{1.95}O_4$ as a cathode and Li metal as an anode. The bilayer separator contains a polyfluorene polymer in contact with the cathode and poly(3-butylthiophene) (P3BT) next to the anode. A modified cell configuration that lowers the internal resistance of the separator during normal operation is also described.

Experimental

A neutral P3BT with a 97% head to tail regiospecific conformation was purchased from Aldrich Chemical Co., Inc. A neutral poly(9,9-dioctylfluorene) end-capped with dimethylphenyl groups (PFO-DMP, Mw = 40,000–120,000) was purchased from American Dye Source, Inc. The polymers were used as received. Samples for cyclic voltammetry (CV) were prepared by dissolving PFO-DMP in chloroform and casting the solution onto a stainless steel mesh current collector (304 stainless steel, 200 mesh). The polymer loading was 0.8 mg over a geometric area of 2.6 cm^2. The polymer-coated working electrode was mounted in a single compartment, three-electrode cell with Li metal as counter and reference electrodes.

Polymer composite separators were prepared by impregnating commercial polypropylene membranes with a 0.02 M solution of PFO-DMP or P3BT in $CHCl_3$/DMF, as described previously.[6] Three types of membrane substrates were used: Celgard 2500 microporous membrane (25 μm thick, 55% porosity), Viledon (Freudenberg) nonwoven membrane (175 μm thick, 55% porosity), and Tapyrus meltblown membrane (65 μm thick, 70% porosity) from Tapyrus Co. Ltd. The polymer loading was 140 $\mu g\ cm^{-2}$.

The $Li_{1.05}Mn_{1.95}O_4$ cathode laminates contained 84 wt % $Li_{1.05}Mn_{1.95}O_4$ powder (Toda M08), 4 wt % Shawinigan carbon black (Chevron), 4 wt % graphite (SFG-6, Timical), and 8 wt % poly(vinylidene fluoride) binder (Kureha) on aluminum foil. Charge–discharge cycling was carried out in "Swagelok"-type cells with $Li_{1.05}Mn_{1.95}O_4$ composite cathodes, polypropylene membranes, Li foil anodes, and stainless steel current collectors. In overcharge-protected cells, polymer composite membranes were used in place of virgin polypropylene membranes. Low temperature experiments were carried out in a Thermotron environmental chamber (model S1.2, Thermotron Industries, Inc.). The temperature was reduced from 25 to −20°C in five steps, with data taken at 25, 20, 10, 0, −10, and −20°C. The cell was held at each temperature for 1 h before testing.

The electrolyte used in the ambient temperature experiments was 1.0 M $LiPF_6$ in 1:1 propylene carbonate (PC) and ethylene carbonate (EC) and was purchased from Ferro Corporation. For the low temperature experiments, an electrolyte 1.0 M $LiPF_6$ in 1:1:3 PC, EC, and dimethyl carbonate (DMC) was provided by the Army Research Laboratory. All cells were assembled in an inert atmosphere glove box with an oxygen content of <1 ppm and water of <2 ppm. X-ray diffraction (XRD) patterns were collected in reflection mode using a Panalytical Xpert Pro diffractometer equipped with monochromatized Cu Kα radiation. The scan rate was 0.0025°/s from 10 to 70° 2θ in 0.01° steps.

Results and Discussion

Room-temperature overcharge protection.— Owing to their low cost, low toxicity, and high rate capability, spinel-type lithium manganese oxides are among the most promising cathode materials for rechargeable lithium batteries. Because the stoichiometric spinel $LiMn_2O_4$ exhibits significant capacity fading during charge/discharge cycling, excess Li is often introduced to improve the cycling stability.[10] The electrode typically operates in a potential win-

* Electrochemical Society Active Member.
z E-mail: gchen@lbl.gov

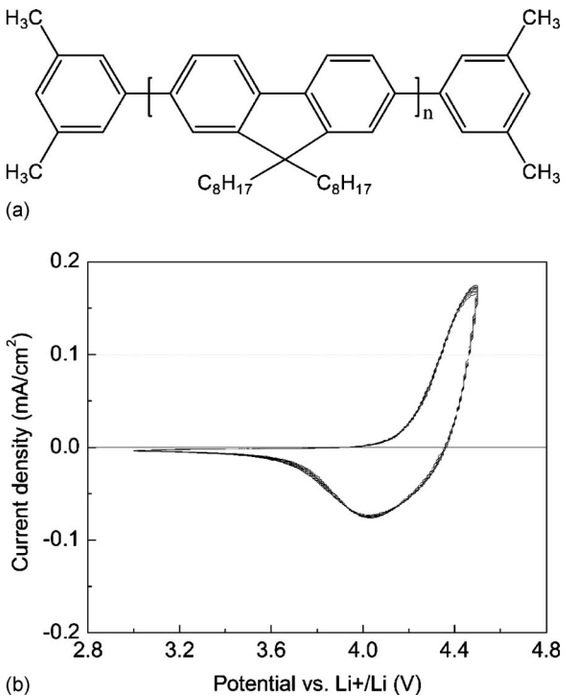

Figure 1. (a) Structure of PFO-DMP and (b) cyclic voltammogram of PFO-DMP in 1.0 M $LiPF_6$ in 1:1 EC:PC. Scan rate of 5 mV s^{-1}, Li foil counter, and reference electrodes.

dow of 3.5–4.3 V and is quite susceptible to overcharge damage, which can result in irreversible structural changes.[11,12] To provide overcharge protection for this material without sacrificing capacity, an electroactive polymer operating just above 4 V is required.

Substituted polyfluorenes have emerged as an important class of electroactive polymers. Their efficient electroluminescence coupled with high charge carrier mobility and good processability has made them attractive for use in organic light emitting diodes.[13,14] Functional characteristics of the polymers, such as intrinsic conductivity, electronic structure, chemical and electrochemical stability, and solubility in organic solvents, are adjustable through the variation of substituent groups. A range of substituted polyfluorenes is commercially available. PFO-DMP (Fig. 1a) was used for this study because of its good solubility in $CHCl_3$ and its measured rapid increase in electronic conductivity upon oxidation. Figure 1b shows a cyclic voltammogram of the polymer at room temperature. A single redox couple, reflecting the oxidation/reduction of the polymer with simultaneous intercalation and deintercalation of PF_6^- anions, was observed when the potential was swept between 3.0 and 4.5 V. The onset oxidation potential was 4.15 V, suggesting that it is suitable for the protection of $Li_{1.05}Mn_{1.95}O_4$ cells. The polymer showed good stability in the electrolyte, as no changes were observed in the CV after 10 cycles.

An overcharge-protected cell, with PFO-DMP coated on a Viledon nonwoven membrane as the high voltage composite separator and P3BT on a Celgard 2500 membrane as the low voltage composite separator, was assembled and tested at room temperature. The nonwoven membrane (Fig. 2a) was chosen to support the high voltage polymer because it possesses a network of long polypropylene fibers and a more open pore structure compared to the microporous membrane (Fig. 2b). It allows for a uniform distribution of PFO-DMP on the internal membrane surfaces and produces a highly porous composite membrane that promotes good utilization of the electroactive polymer (Fig. 2c) and high ion conductivity in the separator. P3BT, with an onset oxidation potential of 3.2 V,[6] was coated onto a Celgard microporous membrane (used to prevent

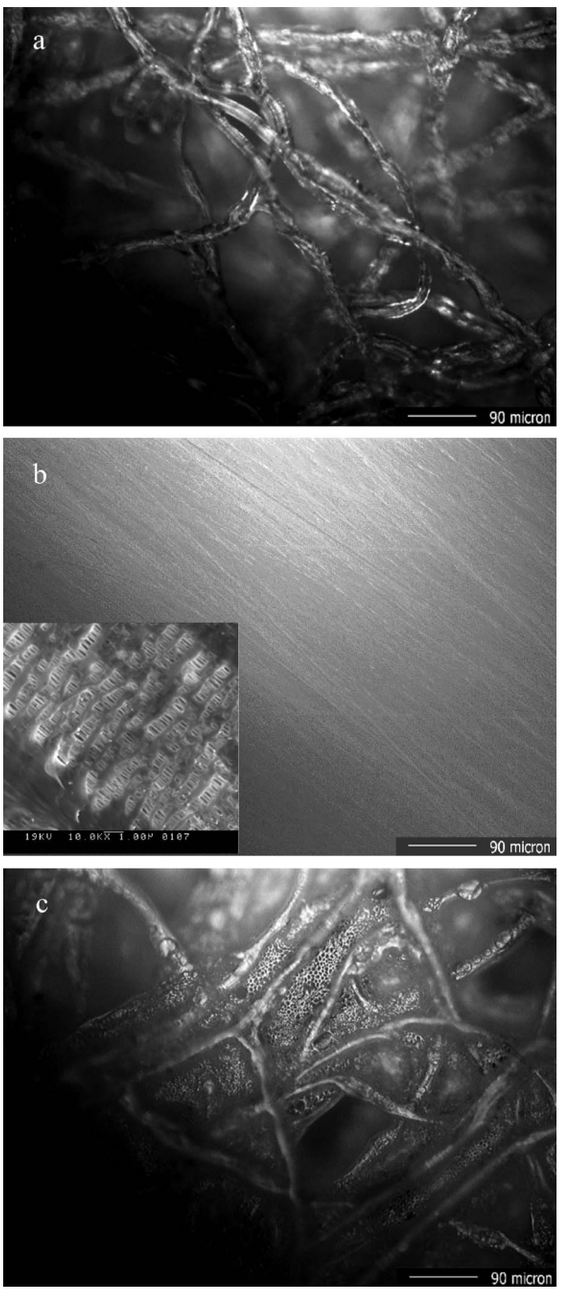

Figure 2. SEM images of (a) Viledon nonwoven membrane, (b) Celgard 2500 membrane, and (c) PFO-DMP-impregnated Viledon membrane.

lithium dendrite penetration) and placed next to the anode. The high voltage PFO-DMP composite determines the electrochemical characteristics of the internal short, while the low voltage P3BT composite protects PFO-DMF from degradation at low voltages close to the anode.

Galvanostatic charge and discharge profiles for the protected $Li_{1.05}Mn_{1.95}O_4$–Li cell are shown in Fig. 3a. At a current density of 0.063 mA/cm^2 (C/6), the cell voltage gradually increased to 4.3 V as the $Li_{1.05}Mn_{1.95}O_4$ cathode was charged. The polymer then began to become conductive, allowing the potential to fall very slightly as it carried most of the charging current until it reached the charging time limit. The cell was overcharged by 20% and then discharged to 3.5 V (Fig. 3b). In each cycle, the polymer short was generated at the end of charging and was then removed during discharging. The

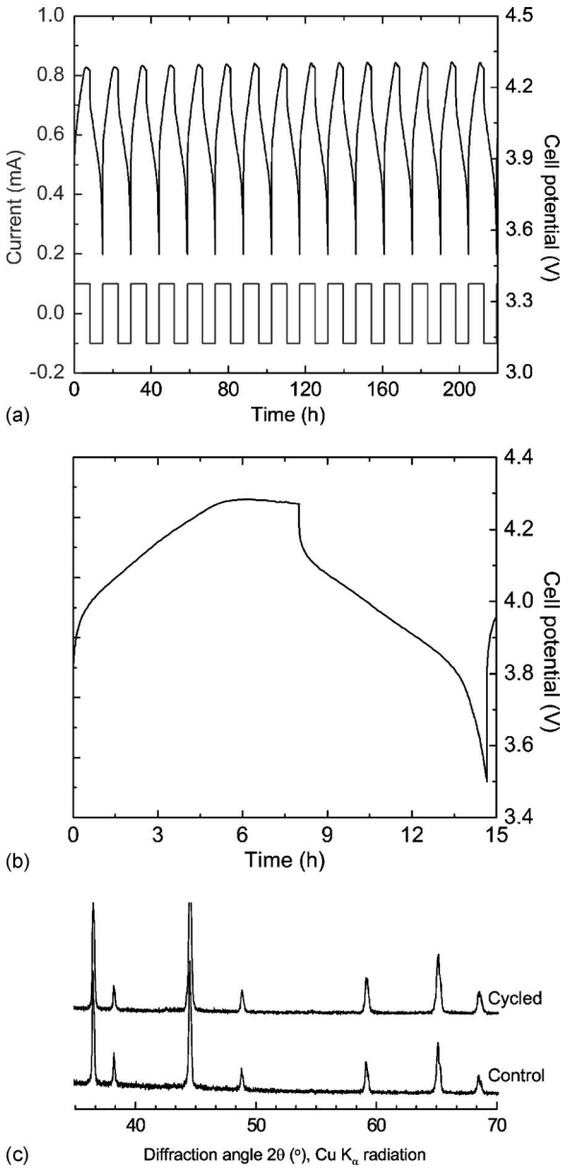

Figure 3. (a) Charge–discharge cycling of a $Li_{1.05}Mn_{1.95}O_4$–Li cell protected with a PFO-DMP Viledon composite and a P3BT Celgard composite; (b) expanded view of the first cycle voltage profile of the protected cell; and (c) XRD patterns of $Li_{1.05}Mn_{1.95}O_4$ electrodes.

protection was highly reversible, as the charge and discharge capacity of the cell remained constant for more than 20 cycles. The XRD pattern of this electrode is shown in Fig. 3c, along with that of the control electrode that was charged once to 4.3 V. The XRD patterns are essentially identical, indicating that the two electrodes were at the same state of charge (SOC) and that no structural changes had occurred in the protected electrode.

For comparison, an unprotected cell with a $Li_{1.05}Mn_{1.95}O_4$ cathode, an uncoated Celgard 2500 separator, and a Li anode was charged at a constant current density of 0.063 mA/cm^2 (C/6) and then held at 4.3 V for 5 h to simulate the cycling profile of the protected cell. The charge–discharge performance is shown in Fig. 4a. One can see that without polymer protection, the charging current gradually decreased during the constant voltage holding at 4.3 V. The capacity of the cell faded quickly as its ability to pass current decreased due to the overcharging abuse. After the final overcharging cycle, the cell was allowed to rest for 2 h and was then disas-

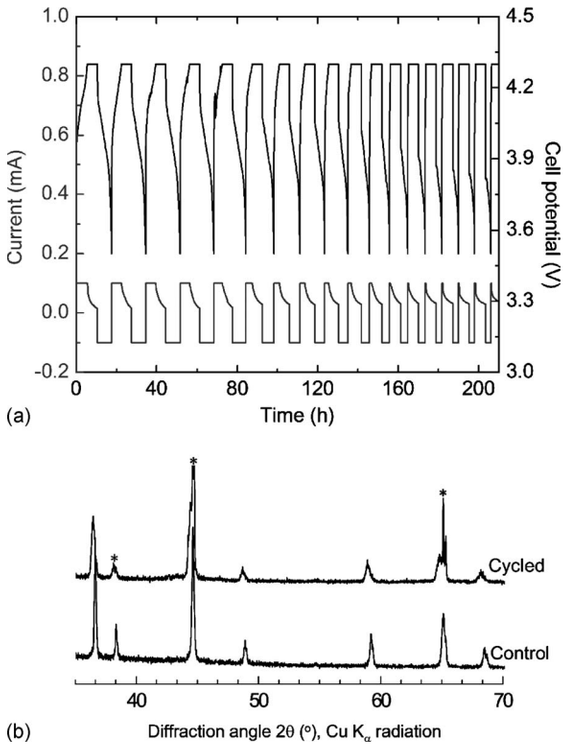

Figure 4. (a) Charge–discharge cycling of an unprotected $Li_{1.05}Mn_{1.95}O_4$–Li cell and (b) XRD patterns of $Li_{1.05}Mn_{1.95}O_4$ electrodes. (∗) indicates peaks from Al sample holder.

sembled in the glove box. The cathode was removed and rinsed thoroughly with DMC to remove the electrolyte residue, then dried in the glove box and examined by XRD. Figure 4b shows the XRD pattern of the charged cathode from the unprotected cell, removed after 18 cycles. Compared to a control electrode that was charged once to 4.3 V at the same charging rate of C/6, the cycled electrode shows significant peak broadening, indicating structural degradation in the material. The peaks of the spinel phase are also at lower diffraction angles compared to those from the control electrode. Because the peaks shift continuously to higher diffraction angles with decreasing lithium content in $Li_{1.05}Mn_{1.95}O_4$,[15] this suggests that the

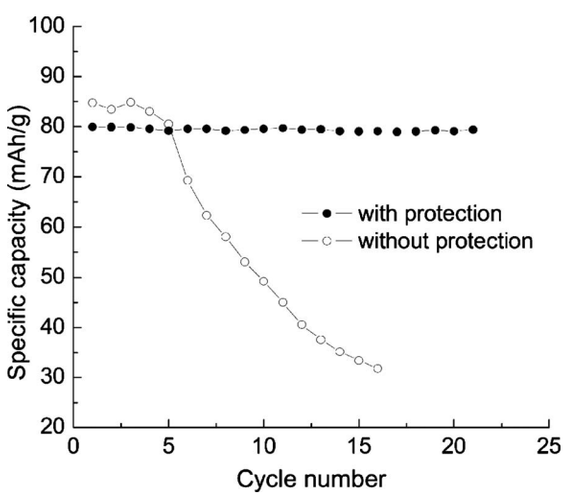

Figure 5. Cycling performance of the protected and unprotected $Li_{1.05}Mn_{1.95}O_4$–Li cells.

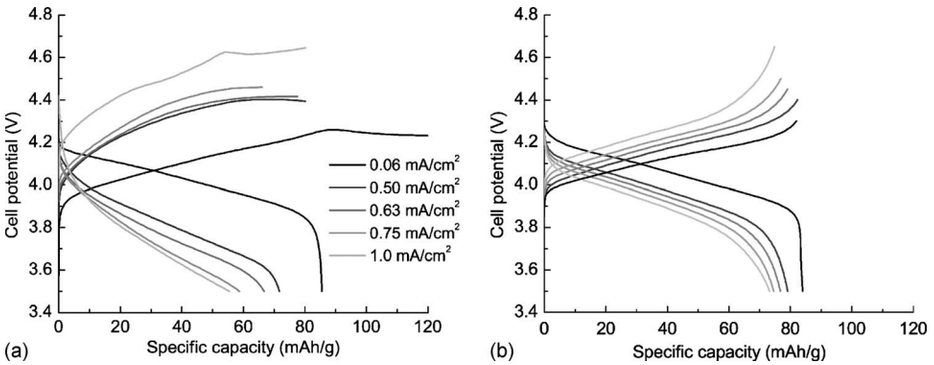

Figure 6. Rate performance of $Li_{1.05}Mn_{1.95}O_4$–Li cells: (a) Protected with a PFO-DMP Viledon composite and a P3BT Celgard composite and (b) unprotected.

cycled electrode is at a lower SOC than that expected at 4.3 V, possibly due to particle isolation within the electrode. Alternatively, the peak shifts may indicate structural changes at the unit cell level.

The discharge capacities of the protected and unprotected cells are shown in Fig. 5. The protected cell maintained its discharge capacity of 80 mAh/g for many cycles, while the unprotected cell quickly lost capacity due to overcharging.

Rate capability of overcharge protection.— Electroactive polymers have the ability to switch rapidly between conductive and insulating states and sustain current densities of as high as 300 mA/cm^2.[7] The current carrying properties of composite membranes coated with electroactive polymers are influenced by other factors, such as the loading of the polymer, the morphology of the deposited polymer, the porosity of the composite, and the availability of doping anions from the electrolyte.

Figure 6 compares the room-temperature rate performance of a plain $Li_{1.05}Mn_{1.95}O_4$–Li cell and a cell protected by the PFO-DMP and P3BT composite separators. Both cells were charged and discharged at current densities of 0.06 (C/6), 0.50 (1.3C), 0.63 (1.7C), 0.75 (2C), and 1.0 mA/cm^2 (2.7C), each for five cycles before moving on to the next higher rate. For the protected cell (Fig. 6a), a steady-state potential was reached and maintained at each cycling rate, indicating that a short was establish and maintained by the conducting polymers. The steady-state potential increased with the charging rate, resulting in the increased oxidation (and electronic conductivity) of the polymers.[7] At a current density of 1.0 mA/cm^2 (2.7 C), the separator was able to maintain a voltage of 4.6 V. In this configuration, however, a steady-state potential could not be maintained above 1.0 mA/cm^2.

The voltage profile of the unprotected cell, which had its upper cutoff voltage set at the steady-state potential of the protected cell for each charge/discharge rate (Fig. 6b), shows less polarization than the protected cell, especially at high rates. The capacity of the protected cell also decreased more rapidly with increasing rate. This is due to the higher internal resistance in the protected cell. While the normal cell contains only a single 25 μm separator, the protected cell has two layers of coated separators with a total thickness of 200 μm.

Low temperature overcharge protection.— At low temperatures, lithium metal can plate on the anode during overcharging, raising safety concerns and causing capacity losses.[16-20] Cells are also more likely to be overcharged due to the increase in cell resistance. The low temperature performance of a $Li_{1.05}Mn_{1.95}O_4$–Li cell protected by the combination of a PFO-DMP Viledon composite and a P3BT Celgard composite is shown in Fig. 7. When charged and discharged at C/6 rate (0.06 mA/cm^2), the cell was reversibly protected at each temperature, ranging from 25 to −20°C. As the temperature decreased, the potential at which the short was initiated increased, mainly due to decreased ion mobility. At each temperature, the short persisted and improved with time, as more of the polymers became conducting. A significant capacity loss occurred below −10°C, as the electrolyte began to solidify and cell resistance increased. At −20°C, the cell was still protected, even though the discharge capacity was very small due to the high polarization of the electrolyte.

Improved rate and low temperature performance with a modified cell configuration.— To decrease the internal resistance of the protected cells, an alternative configuration (Fig. 8) with the electroactive polymers placed outside of the active electrode area was adapted. A different substrate, "Tapyrus" meltblown membrane with 70% porosity and 65 μm thickness, was also used to support the PFO-DMP polymer to better match in thickness. A $Li_{1.05}Mn_{1.95}O_4$–Li cell was assembled with a PFO-DMP-coated Tapyrus membrane and a P3BT-coated Celgard membrane placed in parallel to the cell (in this case, occupying 50% of the current collector area). An untreated Celgard was used as a separator between the cathode and anode. The performance of this cell at charge/discharge current densities of 0.25 (C/1.5), 0.375 (C), 0.50 (1.3C), 0.75 (2C), 1.0 (2.7C), and 1.125 mA/cm^2 (3C) is shown in Fig. 9. The protected cell was able to reach and maintain a steady-state potential for charging rates of as high as 3C. Compared with the data in Fig. 6a, there is a slower increase in the steady-state potential with rate, and the cell was able to maintain at 3C overcharging at 4.3 V. The voltage profile also indicates lower internal resistance, and the discharge capacity remained nearly unchanged with the increasing current density.

The low temperature performance was also examined with the parallel configuration, as shown in Fig. 10. At a C/6 rate, a steady-state potential was reached at each temperature from 25 to −20°C (Fig. 10a). Although, as before, the capacity gradually decreased with decreasing temperature; the change was less significant. The

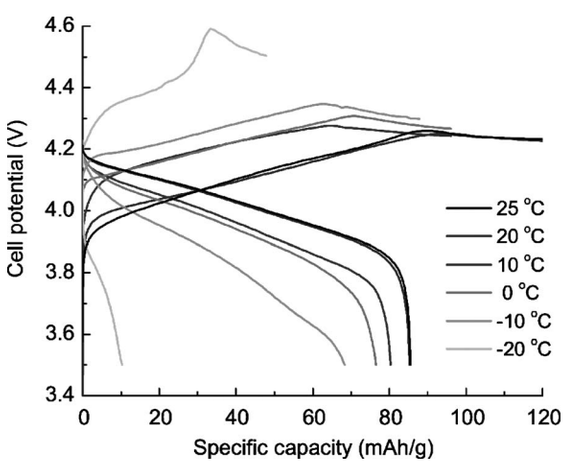

Figure 7. Low temperature performance of a $Li_{1.05}Mn_{1.95}O_4$–Li cell protected with a PFO-DMP Viledon composite and a P3BT Celgard composite.

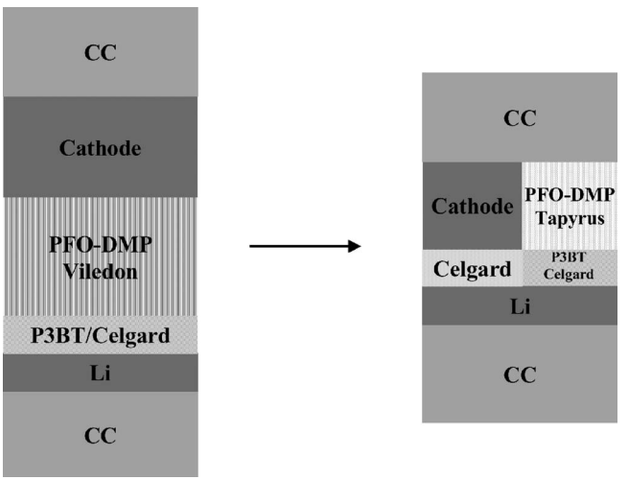

Figure 8. Modified cell configurations for overcharge protection.

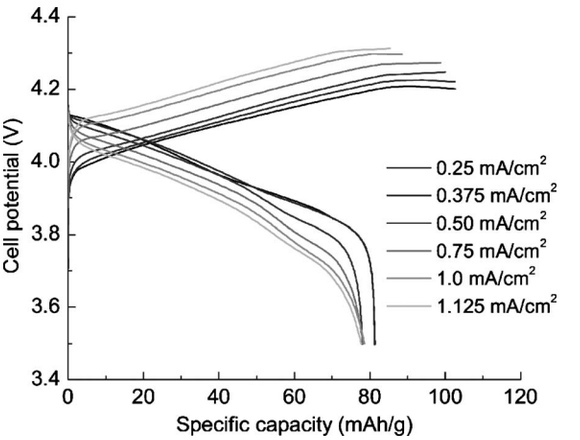

Figure 9. Rate performance of a protected $Li_{1.05}Mn_{1.95}O_4$–Li cell with the cell configuration.

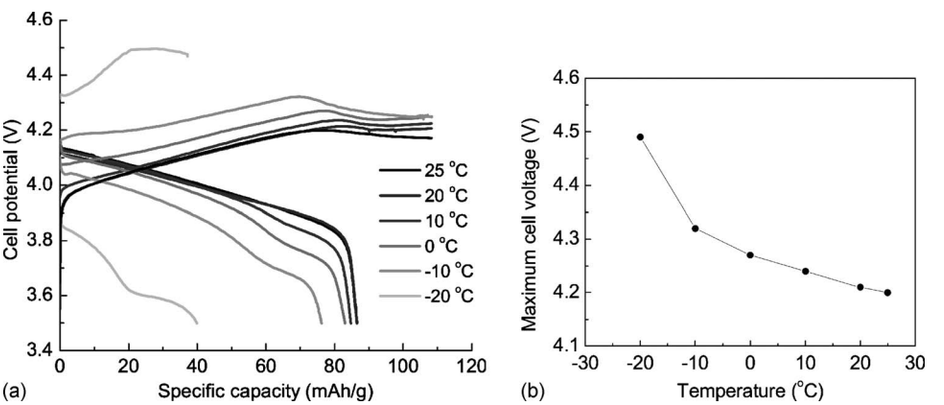

Figure 10. (a) Low temperature performance of a protected $Li_{1.05}Mn_{1.95}O_4$–Li cell with the cell configuration and (b) onset protection potential at different temperatures.

greatest capacity reduction occurred at −20°C, where the cell resistance increased drastically due to the increase in electrolyte viscosity. The onset protection potential increased with decreasing temperature (Fig. 10b), and the cell was protected at 4.5 V at −20°C.

This modified configuration may be implemented in larger battery cells, which have uncoated current collector areas that are designated for tabs. As the loading of the polymer is no longer limited by the separator porosity in this approach, it is possible to use a smaller, denser, and more conductive internal shunt between the two electrodes at the tabbed edges. Future work will aim to optimize polymer morphology to increase its utilization and sustainable current density and to investigate other cell configurations to maximize protection with minimum added cost.

Conclusions

A bilayer configuration consisting of PFO-DMP and P3BT composite separators was used for overcharge protection in $Li_{1.05}Mn_{1.95}O_4$–Li cells. Although this arrangement provided overcharge protection at 2.7 C and at −20°C, substantial internal resistance and capacity losses were observed under these conditions. A modified cell configuration with polymer composites placed next to the electrode assembly was developed, which significantly lowered the internal resistance and provided overcharge protection at a rate up to 3C. The capacity loss at high rate and low temperatures were also significantly lower.

Acknowledgments

We thank Celgard Inc., Freudenberg and Tapyrus Co. Ltd. for providing membranes. This work was supported by the Assistant Secretary for Energy Efficiency and Renewable Energy, Office of Vehicle Technologies of the U.S. Department of Energy under contract no. DE-AC02-05CH11231.

Lawrence Berkeley National Laboratory assisted in meeting the publication costs of this article.

References

1. S. R. Narayanan, S. Surampudi, A. I. Attia, and C. P. Bankston, *J. Electrochem. Soc.*, **138**, 2224 (1991).
2. T. J. Richardson and P. N. Ross, *J. Electrochem. Soc.*, **143**, 3992 (1996).
3. M. Adachi, K. Tanaka, and K. Sekai, *J. Electrochem. Soc.*, **146**, 1256 (1999).
4. J. Chen, C. Buhrmester, and J. R. Dahn, *Electrochem. Solid-State Lett.*, **8**, A59 (2005).
5. M. S. Ding, K. Xu, S. S. Zhang, K. Amine, G. L. Henriksen, and T. R. Jow, *J. Electrochem. Soc.*, **148**, A1196 (2001).
6. G. Chen and T. J. Richardson, *Electrochem. Solid-State Lett.*, **7**, A23 (2004).
7. G. Chen, K. E. Thomas-Alyea, J. Newman, and T. J. Richardson, *Electrochim. Acta*, **50**, 4666 (2005).
8. K. E. Thomas-Alyea, J. Newman, G. Chen, and T. J. Richardson, *J. Electrochem. Soc.*, **151**, A509 (2004).
9. G. Chen and T. J. Richardson, *Electrochem. Solid-State Lett.*, **9**, A24 (2006).
10. Y. Gao and J. R. Dahn, *J. Electrochem. Soc.*, **143**, 1783 (1996).
11. J. M. Tarascon, W. R. Mckinnon, F. Coowar, T. N. Bowmer, G. Amatucci, and D. Guyomard, *J. Electrochem. Soc.*, **141**, 1421 (1994).
12. S. J. Wen, T. J. Richardson, L. Ma, K. A. Striebel, P. N. Ross, and E. J. Cairns, *J. Electrochem. Soc.*, **143**, L136 (1996).

13. Y. Kervella, M. Armand, and O. Stéphan, *J. Electrochem. Soc.*, **148**, H155 (2001).
14. K.-H. Weinfurtner, H. Fujikawa, S. Tokito, and Y. Taga, *Appl. Phys. Lett.*, **76**, 2502 (2000).
15. H. Huang, C. A. Vincent, and P. G. Bruce, *J. Electrochem. Soc.*, **146**, 3649 (1999).
16. J. Fan and S. Tan, *J. Electrochem. Soc.*, **153**, A1081 (2006).
17. H.-P. Lin, D. Chua, M. Salomon, H.-C. Shiao, M. Hendrickson, E. Plichta, and S. Slane, *Electrochem. Solid-State Lett.*, **4**, A71 (2001).
18. M. C. Smart, B. V. Ratnakumer, L. Whitcanack, K. Chin, M. Rodriguez, and S. Surampudi, *IEEE Aerosp. Electron. Syst. Mag.*, **17**, 16 (2002).
19. A. N. Jansen, D. W. Dees, D. P. Abraham, K. Amine, and G. L. Henriksen, *J. Power Sources*, **174**, 373 (2007).
20. S. S. Zhang, K. Xu, and T. R. Jow, *J. Power Sources*, **160**, 1349 (2006).